# Large Eddy Simulation and experimentation in an enclosed rotor-stator flow

Eric Séverac, Sébastien Poncet, Eric Serre, Marie-Pierre Chauve

# Large Eddy Simulation and experimentation in an enclosed rotor-stator flow

**Eric Séverac*, Sébastien Poncet*[+], Eric Serre*, Marie-Pierre Chauve‡**
**Laboratoire MSNM-GP, UMR 6181 CNRS - Universités d'Aix-Marseille*
*IMT La Jetée, Technopôle Château-Gombert, 38 rue F. Joliot-Curie. 13451 Marseille cedex 20 – France*
*[+]poncet@l3m.univ-mrs.fr*
*‡IRPHE, UMR 6594 CNRS - Universités d'Aix-Marseille*
*Technopôle Château-Gombert, 49 rue F. Joliot-Curie. 13384 Marseille – France*

## Abstract:

*Comparisons between Large Eddy Simulation (LES) and velocity measurements have been performed for the turbulent flow in a real shrouded rotor-stator configuration. To investigate turbulent flow regimes, Séverac et al.(2006) have developed a stabilization technique, called SVV (Spectral Vanishing Viscosity), which exhibits the properties of preserving the spectral accuracy of the approximation used in direct numerical simulation (DNS). Thus, numerical results and experimental data have been favourably compared for a large range of the rotational Reynolds number $10^5 \leq Re=\Omega b^2/\nu \leq 10^6$ in an annular cavity of curvature parameter $Rm=(b+a)/(b-a)=1.8$ and of aspect ratio $G=(b-a)/h=5$, where a and b are respectively the inner and outer radii of the rotating disk and h is the interdisk spacing. Coherent vortices have been identified numerically in both boundary layers using the Q-criterion of Hunt et al. (1988).*

## Résumé:

*Cet article propose une étude numérique et expérimentale de l'écoulement turbulent dans une cavité rotor-stator fermée. Les résultats d'une Simulation des Grandes Echelles (LES) sont comparés à des mesures de vitesse par anémométrie laser Doppler à deux composantes. Le code LES est basé sur une méthode de Viscosité Spectrale Evanescente (notée SVV) développée par Séverac et al. (2006) qui permet de conserver la convergence spectrale d'une simulation numérique directe (DNS). On considère une cavité de grand rapport d'aspect $G=(b-a)/h=5$ et de rayon de courbure $Rm=(b+a)/(b-a)=1.8$, où a et b sont les rayons intérieur et extérieur du rotor et h l'espace interdisque. Les approches numérique et expérimentale sont en bon accord pour la gamme de nombre de Reynolds $10^5 \leq Re=\Omega b^2/\nu \leq 10^6$ considérée. Le critère Q défini par Hunt et al. (1988) a permis de mettre en évidence numériquement les structures turbulentes présentes dans les couches limites attachées aux disques.*

**Keywords: rotor-stator flow; large eddy simulation; spectral vanishing viscosity**

## 1 Introduction

Rotating disk flows have been the subject of a constant interest because of their relevance for the turbine engineering field. The rotor-stator problem has also proved a fruitful means of studying turbulence in confined rotating flows. Rotating disk flows are indeed among the simplest flows where the boundary layers are three-dimensional and they are therefore well suited for studying the effects of mean flow three-dimensionality on the turbulence.

The present study concerns a Batchelor type of flow with two boundary layers separated by a central rotating core. Experiments of Itoh *et al.* (1992) have revealed that transition to turbulence first appears within the Bödewadt layer on the stator, even though the Ekman layer along the rotor remains laminar. They reported a turbulent regime occurring along the stator at $Re_r=\Omega r^2/\nu=8\times10^3$ (r the local radius), while along the rotor, turbulence develops later at $3.6\times10^5 < Re_r < 6.4\times10^5$ (G=12.5). Differences in turbulence characteristics between the rotor and the stator have been attributed to the effects of the radial convective transport of turbulence.

The structure of these flows is highly complex involving laminar, transitional and turbulent flow regions. Moreover, because of confinement, flow curvature and rotation effects, the turbulence is strongly inhomogeneous and anisotropic. Consequently, these flows are very challenging for turbulence modelling. The model must be able to solve the region of low Reynolds number near the disks and in the core of the flow and to predict precisely the location of the transition to turbulence, even though the transition process is bounded by instabilities. One of the most important failures of eddy viscosity models in predicting this type of flow is an overestimate of the extent of the relaminarized zone close to the axis, leading to erroneous Ekman layer predictions. Second moment closures provide a more appropriate level of modelling to predict such complex flows (Poncet et *al.* 2005), but even if they provide a satisfactory Reynolds stress behaviour, they fail to predict low Reynolds number regions.

Consequently, the LES constitutes a valuable way to compute such flows. To our knowledge, there exist only two studies of rotating disk flows using LES. Wu & Squires (2000) have been the first to develop LES to predict the statistically three-dimensional turbulent boundary layer over a free rotating disk at Re = $6.5\times10^5$. Their results from three dynamical subgrid models have offered new evidence to support the observations of Littell and Eaton (1994) that streamwise vortices with the same sign as the mean streamwise vorticity are mostly responsible for strong sweep events, while streamwise vortices having opposite sign to the mean streamwise vorticity promote strong ejections. Andersson & Lygren (2006) performed ``wide-gap" and ``narrow-gap" LES in an idealized open rotor-stator cavity for Reynolds numbers up to Re = $1.6\times10^6$ to investigate the degree of three-dimensionality in the boundary layers. Their results support also the conclusions of Littell and Eaton (1994) and Wu and Squires (2000).

## 2 Experimental set-up

The cavity is composed of two smooth disks of radius b=140mm, one rotating at an uniform angular velocity $\Omega$ (rotor), one being at rest (stator). The disks are delimited by an inner cylinder (the hub) of radius a=40 mm attached to the rotor and by an outer stationary casing (the shroud). The stator is located at z*=z/h=1 and the rotor at z*=0. The cavity is filled up with water maintained at a constant temperature 20°C.

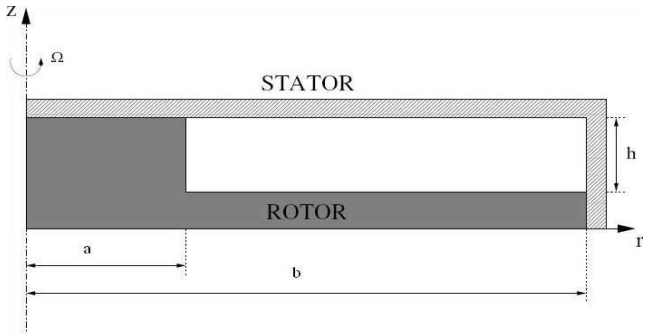


FIG. 1 – Rotor-stator cavity with relevant notation.

The measurements are performed using a two component laser Doppler anemometer (LDA). The LDA technique is used to measure from above the stator the mean radial $V_r$ and tangential $V_\theta$ velocity components as well as the associated Reynolds stress tensor components in a vertical plane (r,z): $R^*_{rr} = \overline{v_r'^2}/(\Omega r)^2$, $R^*_{\theta\theta} = \overline{v_\theta'^2}/(\Omega r)^2$ and $R^*_{r\theta} = \overline{v_r' v_\theta'}/(\Omega r)^2$. This method is based on the accurate measurement of the Doppler shift of laser light scattered by small particles (Optimage PIV Seeding Powder, 30 μm) carried along with the fluid. About 5000 validated data are necessary to obtain the statistical convergence of the measurements.

## 3 The numerical approach

The incompressible fluid motion is governed by the 3D Navier-Stokes equations written in the velocity-pressure formulation together with appropriate boundary and initial conditions. A cylindrical coordinate system (r, θ, z) is used. The scales for the dimensionless variables of space, time and velocity are h/2, $\Omega^{-1}$, Ωb, respectively. The temporal scheme is second-order semi-implicit combining an implicit second order backward Euler scheme for the diffusive terms and an explicit Adams-Bashforth extrapolation for the non-linear convective terms. A collocation Chebychev approximation is used in both radial and axial directions associated with Gauss-Lobatto points. A standard Fourier-Galerkin approximation is employed in the tangential direction. Finally, a full diagonalization technique is used for solving a set of 2D uncoupled Helmholtz and Poisson problems for each Fourier modes (Serre *et al.* 2002).

The LES is performed using a Spectral Vanishing Viscosity (SVV) technique (Séverac *et al.* 2006). A viscosity kernel operator, only active for high wave numbers of the numerical approximation, is incorporated in the Helmholtz equations of velocity prediction. This operator, which stabilizes the solution by increasing the dissipation near the cut off frequency, is defined as:

$$\widetilde{\Delta}V_N \equiv \nabla\cdot\left((\Delta V_N)\times Q_N\right),\ \text{with}\ Q_N = \text{diag}\left\{Q^i_{N_i}\right\} \tag{1}$$

where the 1D operator is only defined in spectral space as a $C^\infty$ smooth function:

$$\hat{Q}^i_{N_i}(\omega) = \varepsilon^i_{N_i}.\chi_{]\omega^i_T;\omega^i_c]}.e^{-\left(\frac{\omega^i_c-\omega}{\omega^i_T-\omega}\right)^2},\ \text{with}\ \varepsilon^i_{N_i} = O\left({\omega^i_c}^{-1}\right)\&\ \omega^i_T = O\left({\omega^i_c}^{-1/2}\right) \tag{2}$$

$Q_N$ denotes the 3D SVV operator composed of three 1D SVV operators $Q^i_{N_i}$ with i=1,2,3 corresponding to the (r, θ, z) directions respectively. The operator is parameterized by $\varepsilon^i_{N_i}$ the maximum of viscosity and $\omega^i_T$ the threshold after which, the viscosity is applied. $\omega^i_C$ is the highest frequency calculated in the i-direction. As the SVV operator is fully linear, it is gathered with the implicit standard diffusion term. Thus, no additional computational cost is required.

The initial condition corresponds to a fluid at rest. No-slip boundary conditions are applied at all walls. The tangential velocity is fixed to zero on the stator and the shroud and to the local disk velocity on the rotor and the hub. The computational parameters used in the present LES are summed up in table 1. Let's notice that the calculations at $Re=10^6$ have been carried out in a half-cavity [0,π], which offers the best arrangement between accuracy and confinement regard.

| Re | $\omega_T$ | $\varepsilon_N$ | grid | δt |
|---|---|---|---|---|
| $10^5$ | 3N/4 (r-direction) | 1/(2N) | 81 | $10^{-4}$ |
| | N/2 (θ-direction) | 1/(2N) | 150 | |
| | √N (z-direction) | 1/(2N) | 49 | |
| $4 \times 10^5$ | 0.8√N | 1/(2N) | 121 | $10^{-4}$ |
| | √N | 1/(2N) | 181 | |
| | √N | 1/(2N) | 65 | |
| $10^6$ | 2√N | 1/N | 151 | $10^{-5}$ |
| | 5√N | 1/N | 241 | |
| | 4√N | 1/N | 81 | |

Table 1 - Computational parameters.

## 4 Results

Note that all the quantities have been normalized by the local rotor velocity Ωr. The statistical data have been averaged both in time and in the homogeneous tangential direction.

Three Reynolds numbers $Re=10^5$, $Re=4\times10^5$ and $Re=10^6$ corresponding to different flow properties have been considered and the results are presented at mid-radius $r^*=(r-a)/(b-a)=0.5$.

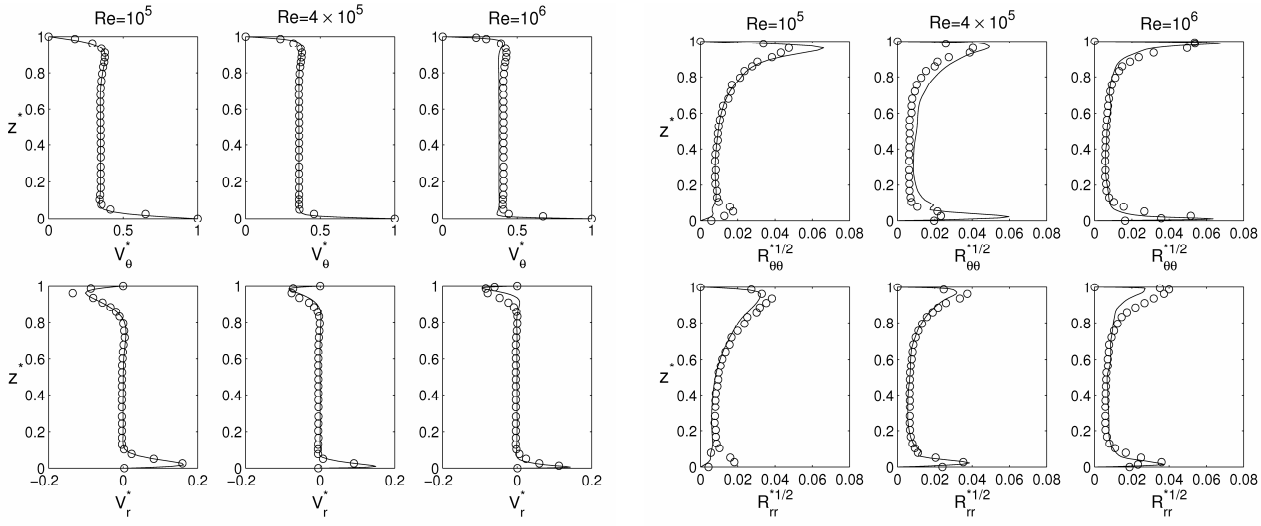


FIG. 2 – Axial profiles of (a) the mean radial and tangential velocity components and of (b) two normal components of the Reynolds stress tensor. Comparisons between numerical (solid lines) and experimental (circles) statistical data at mid-radius.

For all Reynolds numbers considered, the mean flow is of Batchelor type (Fig.2a), with two boundary layers separated by a core in solid body rotation. The mean tangential velocity component in the core, known as the entrainment coefficient of the fluid K, slightly increases with Re from 0.348 at $Re=10^5$ to 0.377 at $Re=10^6$. These values are consistent with the ones measured by Itoh *et al.* (1992). The thickness of the Ekman layer on the rotor, which is known to scale as $\delta=(\nu/\Omega)^{1/2}$, the thickness of the boundary layer over a single rotating disk, decreases with Re by a factor two between $Re=10^5$ and $Re=10^6$. It is characteristic of a rotating boundary layer, which gets turbulent. By conservation of mass, the thickness of the Bödewadt layer on the stator behaves like the Ekman one. Note that the Bödewadt layer is almost twice thicker than the Ekman layer. The agreement between the numerical results and the measurements is very satisfactory for the mean field. The LES catches the main features of turbulent rotor-stator flows such as the thinning of the boundary layers for increasing values of Re. At $Re=10^6$, the simulation slightly underestimates the coefficient K with a difference of 6.33%.

Figure 2b presents the axial variations of two normal Reynolds stress tensor components at mid-radius. An examination of the off-diagonal components from LES results shows that these normal components are dominant. The turbulence is found to be mainly confined in the boundary layers, whereas the core remains laminar whatever the Reynolds number. For the three cases, the numerical profiles fit quite well the velocity measurements both in the boundary layers and in the core. Nevertheless, the LES tends to underestimate the turbulence intensity and especially in the Bödewadt layer for the $R_{rr}$ component. It confirms the results for the mean field as the underestimation of K is characteristic of a lower turbulence level.

At $Re=10^5$, the flow regime is transitional turbulent, characterized by a fully turbulent Bödewadt layer with increasing intensities towards the periphery and a laminar Ekman layer (Fig.2b). This can be seen also from the isosurface plot of the Q-criterion (Hunt et *al.* 1988). On the rotor side (Fig.3a), turbulence originates both on the rotating shroud and on the external cylinder, which confirms the important effects that the cylinders have on the turbulence

characteristics. The rotating hub has a strong destabilizing effect, contrary to the configuration where the hub is stationary (Serre et *al.* 2002). For $Re=4\times10^5$, the stator (Fig.2b, 3e) is fully turbulent, while the rotor layer (Fig.2b, 3b) is transitional turbulent. At $Re=4\times10^5$, the turbulence intensities are larger on the rotor than on the stator in the LES results, as already mentioned by Lygren & Andersson (2001) using DNS (Fig.2b). It can be attributed to the different closures introduced between the rotating and fixed parts of the cavity in the LES and in the experiments. About 19 spiral arms (Fig.3b) forming a positive angle of 16° with the tangential direction (as they roll up in the rotation sense) appear in the Ekman layer for $0.14\leq r^*\leq0.61$, where the flow is laminar unstable ($89\leq Re_r{}^{1/2}\leq386<500$). These structures are characteristic of the Type I instability (crossflow instability), which plays an important role in the transition process to turbulence. Towards the periphery, the structures get thinner and more axisymmetric. It is characteristic of a turbulent flow. At $Re=10^6$ (Fig.2b,3c,3f), the flow gets fully turbulent in both boundary layers.

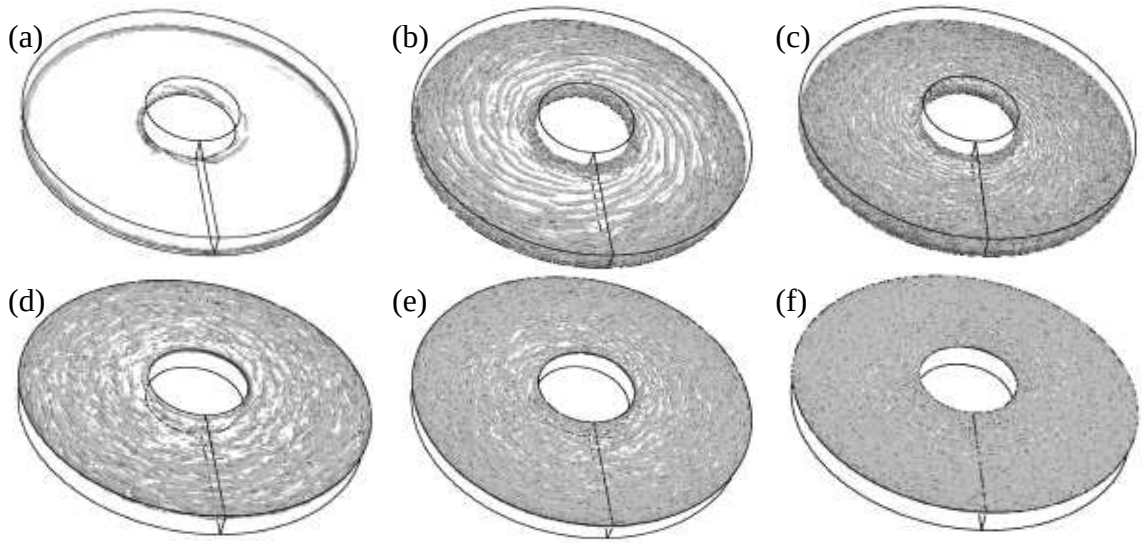


FIG. 3 – Isosurface plot (top view) of the Q-criterion in the Ekman layer (a,b,c) and in the Bödewadt layer (d,e,f) at $Re=10^5$ (a,d), $Re=4\times10^5$ (b,e) and $Re=10^6$ (c,f).

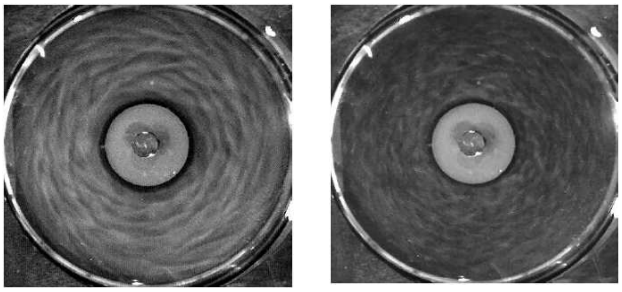

FIG. 4 – Flow visualizations from above the stator for (a) Re=41000 and (b) $Re=10^5$.

To confirm the isosurface plot of the Q-criterion obtained from the LES, some flow visualizations have been performed from above the stator for two Reynolds numbers $Re=4.1\times10^4$ and $Re=10^5$ using a CCD video camera. The cavity has been filled up with water and seeded with reflective particles of kalliroscope (30×6×0.07 μm). During the transition to turbulence, the flow structures are known to evolve from circular rolls to spiral arms. For $Re=4.1\times10^4$ (Fig.4a), the flow structure is already complex but it is still organized by large structures showing spiral

patterns with defects. For $Re=10^5$, the Bödewadt layer is clearly turbulent (Fig.4b) with flow structures much thinner and more aligned on the tangential direction.

## 5 Conclusion

A coupled numerical and experimental investigation of turbulent shrouded rotor-stator flows has been performed. The highly accurate computation of turbulent rotating flows within finite cavity is of interest for both engineering applications (turbomachinaries) and fundamental research, as it is one of the simplest cases where the turbulent boundary layers are three-dimensional. The results of a Large Eddy Simulation using a 3D spectral code stabilized with a Spectral Vanishing Viscosity model have been favourably compared to velocity measurements for both the mean and turbulent fields and Reynolds numbers in the range $[10^5; 10^6]$.

The structure of the mean flow is of Batchelor type with separated boundary layers. For $Re=10^5$, the flow is transitional turbulent: the Bödewadt layer on the stator is turbulent, whereas the Ekman layer on the rotor remains laminar. At $Re=4\times10^5$, both boundary layers are turbulent with increasing turbulence intensities towards the periphery of the cavity. Close to the rotation axis, spiral arm patterns appear along the rotor. For $Re=10^6$, the flow gets fully turbulent. In the Bödewadt layer, the coherent vertical structures, aligned with the tangential direction, get thinner when one increases the Reynolds number.

**Acknowledgements**

The authors acknowledge the IDRIS (CNRS, Orsay) center where the computations have been carried out on the NEC SX-5 (program 060242). The authors are very grateful to Prof. R. Pasquetti (CNRS / Lab. J. Dieudonnée, Nice) and B.E. Launder (Univ. of Manchester) for fruitful diskussions. The work was supported by CNRS in the frame of DFG-CNRS program "LES of complex flows". Support for E. Séverac by a CNRS grant is also acknowledged.

## References

Andersson H.I., Lygren M. (2006), LES of open rotor-stator flow, *Int. J. Heat Fluid Flow* **27**, 551-557

Hunt J.C.R., Wray A., Moin P. (1988) Eddies, stream, and convergence zones in turbulent flows, *Center for Turbulence Research Report*, CTR-S88

Itoh M., Yamada Y., Imao S., Gonda M. (1992), Experiments on turbulent flow due to an enclosed rotating disk, *Exp. Thermal Fluid Sci.* **5**, 359-368

Littell H.S., Eaton J.K. (1994) Turbulence characteristics of the boundary layer on a rotating disk. *J. Fluid. Mech.* **266**, 175-207

Lygren M., Andersson H.I. (2001), Turbulent flow between a rotating and a stationary disk, *J. Fluid Mech.* **426**, 297-326

Poncet S., Chauve M.-P., Schiestel R. (2005), Batchelor versus Stewartson flow structures in a rotor-stator cavity with throughflow, *Phys. Fluids* **17**, 075110

Serre E., Bontoux P., Launder B. (2002), Direct numerical simulation of transitional turbulent flow in a closed rotor-stator cavity, *Flow, Turbulence & Combustion* **60**, 35-50

Séverac E., Serre E., Bontoux P., Launder B.E. (2006), Large eddy simulation of transitional rotor-stator flows using a spectral vanishing viscosity technique, ERCOFTAC Series 10: 217-224. Lamballais, E. (Eds): Direct and Large-Eddy Simulation VI. Springer-Verlag

Wu X., Squires K.D. (2000), Prediction and investigation of the turbulent flow over a rotating disk, *J. Fluid. Mech.* **418**, 231-264